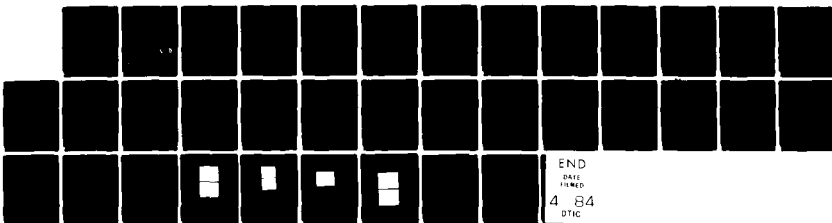


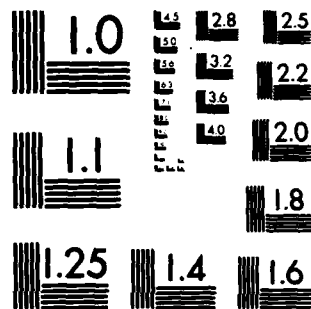
AD-A138 412 TECHNIQUES OF FLASH RADIOMETRY(U) IBM RESEARCH LAB SAN 1/1
JOSE CA W P LEUNG ET AL. 20 JAN 84 RJ-4152 (45940)
N00014-83-C-0170

UNCLASSIFIED

F/G 12/1

NL





MICROCOPY RESOLUTION TEST CHART
NATIONAL BUREAU OF STANDARDS-1963-A

12

SECURITY CLASSIFICATION OF THIS PAGE (When Data Entered)

410

REPORT DOCUMENTATION PAGE

READ INSTRUCTIONS BEFORE COMPLETING FORM

1. REPORT NUMBER 6	2. GOVT ACCESSION NO. AD-A288422	3. RECIPIENT'S CATALOG NUMBER
4. TITLE (and Subtitle) TECHNIQUES OF FLASH RADIOMETRY		5. TYPE OF REPORT & PERIOD COVERED Technical Report
7. AUTHOR(s) W. P. Leung and A C. Tam		6. PERFORMING ORG. REPORT NUMBER
9. PERFORMING ORGANIZATION NAME AND ADDRESS International Business Machines Corp. 5600 Cottle Road San Jose, CA 95193		8. CONTRACT OR GRANT NUMBER(s) N00014-83-C-0170
11. CONTROLLING OFFICE NAME AND ADDRESS Office of Naval Research 800 N. Quincy Street Arlington, VA 22217		10. PROGRAM ELEMENT, PROJECT, TASK AREA & WORK UNIT NUMBERS NR 633-844
14. MONITORING AGENCY NAME & ADDRESS (if different from Controlling Office)		12. REPORT DATE January 20, 1984
		13. NUMBER OF PAGES 26
		15. SECURITY CLASS. (of this report) Unclassified
		15a. DECLASSIFICATION/DOWNGRADING SCHEDULE

16. DISTRIBUTION STATEMENT (of this Report)
This document has been approved for public release and sale; its distribution is unlimited.

17. DISTRIBUTION STATEMENT (of the abstract entered in Block 20, if different from Report)

18. SUPPLEMENTARY NOTES
To be published in Journal of Applied Physics

19. KEY WORDS (Continue on reverse side if necessary and identify by block number)
Radiometry, thermal diffusivity
This document

20. ABSTRACT (Continue on reverse side if necessary and identify by block number)
We analyze, in detail flash radiometry techniques for determining the thermal diffusivity of thin condensed samples. Such techniques rely on the transient infrared radiation from the sample heated by a short-duration pulsed radiation. Exact analytical solution for the conventional transmission measurement (in which the excitation source and the infrared detector are on opposite sides of the sample) as well as the back-scattering measurement (in which the excitation source and detector are on the same side of the sample) are presented with the effect ~~(cont-over)~~

DTIC
ELECTE
FEB 22 1984
S D
E

ADA138412

DTIC FILE COPY

DD FORM 1473 1 JAN 73

EDITION OF 1 NOV 65 IS OBSOLETE S/N 0102-LF-014-6601

SECURITY CLASSIFICATION OF THIS PAGE (When Data Entered)

84 02 17 040

20. (cont)

→ of heat loss neglected. The analysis allows the determination of the thermal diffusivity and the absorption coefficients at the excitation wavelength and at the detecting wavelength of the sample from the experimental data. The effects of excitation pulse duration and finite rise time of the detection system are discussed. Experiments on pulsed radiometry measurements on thin film samples are performed to verify some of these theoretical predictions. Radiation loss and two-dimensional head diffusion loss are shown to be negligible for thin film samples.

DL/413/83/01
GEN/413-2

TECHNICAL REPORT DISTRIBUTION LIST, GEN

	<u>No. Copies</u>		<u>No. Copies</u>
Office of Naval Research Attn: Code 413 800 N. Quincy Street Arlington, Virginia 22217	2	Naval Ocean Systems Center Attn: Technical Library San Diego, California 92152	1
ONR Pasadena Detachment Attn: Dr. R. J. Marcus 1030 East Green Street Pasadena, California 91106	1	Naval Weapons Center Attn: Dr. A. B. Amster Chemistry Division China Lake, California 93555	1
Commander, Naval Air Systems Command Attn: Code 310C (H. Rosenwasser) Washington, D.C. 20360	1	Scientific Advisor Commandant of the Marine Corps Code RD-1 Washington, D.C. 20380	1
Naval Civil Engineering Laboratory Attn: Dr. R. W. Drisko Port Hueneme, California 93401	1	Dean William Tolles Naval Postgraduate School Monterey, California 93940	1
Superintendent Chemistry Division, Code 6100 Naval Research Laboratory Washington, D.C. 20375	1	U.S. Army Research Office Attn: CRD-AA-IP P.O. Box 12211 Research Triangle Park, NC 27709	1
Defense Technical Information Center Building 5, Cameron Station Alexandria, Virginia 22314	12	Mr. Vincent Schaper DTNSRDC Code 2830 Annapolis, Maryland 21402	1
DTNSRDC Attn: Dr. G. Bosmajian Applied Chemistry Division Annapolis, Maryland 21401	1	Mr. John Boyle Materials Branch Naval Ship Engineering Center Philadelphia, Pennsylvania 19112	1
Naval Ocean Systems Center Attn: Dr. S. Yamamoto Marine Sciences Division San Diego, California 91232	1	Mr. A. M. Anzalone Administrative Librarian PLASTE/ARRADCOM Bldg 3401 Dover, New Jersey 07801	1

DL/413/83/01
633/413-2

TECHNICAL REPORT DISTRIBUTION LIST, 633

Dr. Henry Freiser
Chemistry Department
University of Arizona
Tucson, Arizona 85721

Dr. Lynn Jarvis
Code 6170
Naval Research Laboratory
Washington, D.C. 20375

Dr. Gregory D. Botsaris
Department of Chemical Engineering
Tufts University
Medford, Massachusetts 02155

Dr. Richard Hollins
Code 385
Naval Weapons Center
China Lake, California 93555

Dr. J. H. Hargis
Department of Chemistry
Auburn University
Auburn, Alabama 36849

Dr. Christie G. Enke
Department of Chemistry
Michigan State University
East Lansing, Michigan 48824

Dr. Andrew Tam
IBM San Jose
5600 Cottle Road
San Jose, California 95193

Dr. Ronald S. Sheinson
Code 6180
Naval Research Laboratory
Washington, D.C. 20375

Dr. Timothy L. Rose
EIC Laboratories, Inc.
111 Chapel Street
Newton, Massachusetts 02158

OFFICE OF NAVAL RESEARCH
Contract N00014-83-C-0170
Task No. 633-844

TECHNICAL REPORT NO. 6



Techniques of Flash Radiometry

by

W. P. Leung and A. C. Tam

IBM Research Laboratory
San Jose, California 95193

Accession For	
NTIS GRA&I	<input checked="" type="checkbox"/>
DTIC TAB	<input type="checkbox"/>
Unannounced	<input type="checkbox"/>
Justification	
By _____	
Distribution/	
Availability Codes	
Dist	Avail and/or Special
A1	

Reproduction in whole or in part is permitted for
any purpose of the United States Government

This document has been approved for public
release and sale, its distribution is unlimited

RJ 4152 (45940) 1/6/84
Physics

(12)

Research Report

TECHNIQUES OF FLASH RADIOMETRY

W. P. Leung
A. C. Tam

IBM Research Laboratory
San Jose, California 95193

LIMITED DISTRIBUTION NOTICE

This report has been submitted for publication outside of IBM and will probably be copyrighted if accepted for publication. It has been classified as Research Report to allow dissemination of its contents. In view of the transfer of copyright to the outside publisher, its distribution outside of IBM prior to publication should be limited to peer communications and related results. After outside publication, results should be cited only by referring to legally obtained copies of the article (e.g., payment of royalties).

IBM

Research Division
Yorktown Heights, New York • San Jose, California • Zurich, Switzerland

620 27 01 10 29

RJ 4152 (45940) 1/6/84
Physics

TECHNIQUES OF FLASH RADIOMETRY

W. P. Leung*
A. C. Tam

IBM Research Laboratory
San Jose, California 95193

ABSTRACT: We analyze in detail flash radiometry techniques for determining the thermal diffusivity of thin condensed matter samples. Such techniques rely on the transient infrared radiation from the sample heated by a short-duration pulsed radiation. Exact analytical solutions for the conventional transmission measurement (in which the excitation source and the infrared detector are on opposite sides of the sample) as well as the back-scattering measurement (in which the excitation source and the detector are on the same side of the sample) are presented with the effect of heat loss neglected. The analysis allows the determination of the thermal diffusivity and the absorption coefficients at the excitation wavelength and at the detecting wavelength of the sample from the experimental data. The effects of excitation pulse duration and finite rise time of the detection system are discussed. Experiments on pulsed radiometry measurements on thin film samples are performed to verify some of these theoretical predictions. Radiation loss and two-dimensional heat diffusion loss are shown to be negligible for thin film samples.

*Permanent Address: Department of Physics, Chinese University of Hong Kong, Shatin, N.T., Hong Kong

INTRODUCTION

The flash method of measuring thermal diffusivity has attracted widespread interest¹⁻¹⁴ since it was introduced in 1961.^{1,2} The technique relies on the use of a short-duration heat pulse to produce an initial thermal gradient in a sample; subsequently the time development of the temperature at the back surface (or the temperature difference between the front and back surfaces¹³) of the sample is measured using thermocouples. Physical parameters such as thermal diffusivity, heat capacity and thermal conductivity can be obtained by analyzing the shape of the temperature-time curve. However, this method is not a radiometry technique because thermocouple or other temperature measuring device has to be attached to the sample surface. The first flash radiometry measurement was carried out in 1962 by Deem and Wood⁴ who modified the technique of Parker *et al.*¹ For temperature sensing, they used a lead sulfide cell to detect infrared radiation emitted from the backside of the sample. The radiometry technique, which eliminates the use of thermocouple, provides a convenient way for the remote measurement of the thermal diffusivity of materials. This method is particularly attractive for the measurement of samples in vacuum, high pressure, high temperatures and other hostile environments.^{4,7} Since the response time of the infrared detector is usually much faster than that of a thermocouple, data can be collected in a matter of microseconds to milliseconds, depending on the thickness and thermal properties of the sample. This is especially important when the physical properties of the sample are changing with time (*e.g.*, under a phase transition).

The above mentioned transmission radiometry technique is "double-ended" (*i.e.*, the excitation source and the detecting system are on opposite sides of the sample). Recently, we^{15,16} have developed a new back-scattering flash radiometry technique in which the excitation source and the infrared detector are on the same side of the sample. This

"single-ended" (*i.e.*, apparatus only on one side of the sample) back-scattering arrangement can provide measurements of thermal diffusivity and absorption coefficient at the excitation wavelength for a sample without contact. This method is also of vital importance when the back side of the sample is inaccessible so that conventional techniques cannot be applied. Furthermore, any change in the sample surface or substrate conditions can be detected remotely and nondestructively.

Although flash radiometry was developed more than twenty years ago, very little theoretical work has been done on the shape of the infrared signal at the detector. In this paper, we fill this important gap by analyzing this technique theoretically. Exact analytical solutions are given with the heat loss neglected. The effects of the duration of the excitation flash pulse as well as the rise time of the detecting system are investigated. Comparisons with experimental data are made and the effect of heat loss is discussed.

THEORY

In the following discussion, we assume a one-dimensional heat flow model. This assumption is valid when the thickness of the sample is much smaller than the lateral dimensions of the area illuminated by the optical excitation flash. To simplify the mathematical analysis further, we assume the heat loss due to convection and radiation at the sample surfaces and due to lateral conduction to be negligible. However, we shall discuss the effect of heat loss qualitatively in the next section.

In order to get some physical insight in the problem, we first examine the situation where the specimen can be treated as a homogeneous semi-infinite solid. Then we consider the case of a thin sample which resembles our experimental situations.

The evolution of the time and position dependent temperature $\theta(x,t)$ inside the sample generated by the absorption of the flash pulse is governed by the one-dimensional diffusion equation

$$\frac{\partial \theta(x,t)}{\partial t} = D \frac{\partial^2 \theta(x,t)}{\partial x^2}, \quad (1)$$

subject to the adiabatic boundary condition

$$\frac{\partial \theta(x,t)}{\partial x} = 0 \quad (2)$$

at the sample surfaces, where D is the thermal diffusivity of the sample and x is the distance into the sample (with $x=0$ being the irradiated surface).

A. Semi-Infinite Solid

The general solution satisfied by Eqs. (1) and (2) for a semi-infinite solid bound by the plane at $x=0$ and extending to infinity in the direction of positive x is given by Carslaw and Jaeger.¹⁷ If the initial ($t=0$) temperature (above the ambient temperature T_0) inside the sample is $\theta(x,0)$, the subsequent temperature distribution is

$$\theta(x,t) = (4\pi Dt)^{-1/2} \int_0^{\infty} \theta(x',0) \left\{ e^{-\frac{(x-x')^2}{4Dt}} + e^{-\frac{(x+x')^2}{4Dt}} \right\} dx'. \quad (3)$$

In flash radiometry experiments, the heat generated inside the sample due to the absorption of the flash pulse energy is proportional¹⁸⁻²³ to ae^{-ax} at a distance x from the irradiated surface. Hence

$$\theta(x',0) = Aae^{-ax'} \quad (4)$$

where A is a constant dependent on the flash pulse energy and the heat capacity of the sample, and α is the absorption coefficient at the excitation wavelength. Thus the subsequent temperature profile after the excitation is

$$\begin{aligned} \theta(x,t) &= A\alpha(4\pi Dt)^{-1/2} \int_0^{\infty} e^{-\alpha x'} \left\{ e^{-\frac{(x-x')^2}{4Dt}} + e^{-\frac{(x+x')^2}{4Dt}} \right\} dx' \\ &= \left(\frac{A\alpha e^{\alpha^2 Dt}}{2} \right) \left\{ \left[1 + \operatorname{erf} \left(\frac{x-2\alpha Dt}{2\sqrt{Dt}} \right) \right] e^{-\alpha x} \right. \\ &\quad \left. + \left[1 - \operatorname{erf} \left(\frac{x+2\alpha Dt}{2\sqrt{Dt}} \right) \right] e^{\alpha x} \right\} \end{aligned} \quad (5)$$

where erf is the error function. Equation (5) does not take into account the effect of finite pulse width of the excitation pulse. However, this aspect will be discussed later in this section.

The signal $S(t)$ at the infrared detector monitoring the thermal radiation from the front surface is^{15,16,18-23}

$$S(t) = K'\alpha' \int_0^{\infty} \left\{ [T_0 + \theta(x,t)]^4 - T_0^4 \right\} e^{-\alpha' x} dx \quad (6)$$

where $K' = 4\epsilon\sigma$ is a constant,¹⁸ ϵ is emissivity averaged over the detection bandwidth, σ is Stefan-Boltzmann constant, T_0 is the ambient temperature in Kelvin, and α' is the infrared absorption coefficient of the sample averaged over the detection bandwidth. When $\theta(x,t)$ is small compared with T_0 , Eq. (6) can be written as

$$S(t) = K\alpha' \int_0^{\infty} \theta(x,t) e^{-\alpha' x} dx \quad (7)$$

where $K=4K'T_0^3$. Substituting Eq. (5) into (7), and after some mathematical manipulations (see Appendix I), we obtain

$$S(t) = \frac{AK\alpha\alpha'}{\alpha'^2 - \alpha^2} \left\{ \alpha' e^{t/4\tau_\alpha} \left(1 - \operatorname{erf} \sqrt{t/4\tau_\alpha} \right) - \alpha e^{t/4\tau_{\alpha'}} \left(1 - \operatorname{erf} \sqrt{t/4\tau_{\alpha'}} \right) \right\} \quad (8)$$

where $\tau_\alpha = \frac{1}{4\alpha^2 D}$ and $\tau_{\alpha'} = \frac{1}{4\alpha'^2 D}$ are the characteristic time constants of the material corresponding approximately to the times required for the heat to diffuse a distance α^{-1} and α'^{-1} , respectively. For most opaque materials, τ_α and $\tau_{\alpha'}$ are in the range of 10^{-5} to 10^{-8} seconds. Equation (8) is also found to be valid in the limit of α' approaching α (Appendix I).

It is of interest to note that Eq. (8) for the magnitude of the flash radiometry signal contains a coefficient $\alpha\alpha'$. For samples that are either transparent in the excitation wavelength ($\alpha=0$), or in the infrared detection wavelength ($\alpha'=0$), the signal $S(t)$ vanishes. Physically, these can be understood as follows: The first situation ($\alpha=0$) corresponds to no excitation and hence no signal; in the latter case ($\alpha'=0$), the detector sees the summation of all infrared signals from the depth of the sample without being attenuated, which does not change with time if there is no heat loss from the sample.

When the time is small such that $\sqrt{t/4\tau_\alpha} \ll 1$ and $\sqrt{t/4\tau_{\alpha'}} \ll 1$,

$$e^{t/4\tau_\alpha} \left(1 - \operatorname{erf} \sqrt{t/4\tau_\alpha} \right) \approx \left(1 - 2\sqrt{t/4\pi\tau_\alpha} \right)$$

and

$$e^{t/4\tau_{\alpha'}} \left(1 - \operatorname{erf} \sqrt{t/4\tau_{\alpha'}} \right) \approx \left(1 - 2\sqrt{t/4\pi\tau_{\alpha'}} \right).$$

Hence, from Eq. (8), the flash radiometry signal $S(t)$ at small t is given by

$$S(t) \sim 1 - \frac{1}{\sqrt{\pi}} \left(\frac{1}{\sqrt{\tau_a}} + \frac{1}{\sqrt{\tau_a'}} \right) \sqrt{t} \quad (\text{small } t).$$

When $\sqrt{t/4\tau_a} \gg 1$ and $\sqrt{t/4\tau_a'} \gg 1$,

$$e^{t/4\tau_a} (1 - \operatorname{erf} \sqrt{t/4\tau_a}) \approx (\pi t/4\tau_a)^{-1/2}$$

and

$$e^{t/4\tau_a'} (1 - \operatorname{erf} \sqrt{t/4\tau_a'}) \approx (\pi t/4\tau_a')^{-1/2}$$

and thus the signal $S(t)$ is

$$S(t) \sim t^{-1/2} \quad (\text{large } t).$$

Hence, $S(t)$ decays very slowly for large t .

B. Thin Solid Slab

The situation for the diffusion Eq. (1) and boundary condition (2) corresponding to a thin solid slab shown in Fig. 1 is also described by Carslaw and Jaeger.²⁴ If the initial temperature distribution (above ambient temperature T_0) inside the slab is $\theta(x,0)$, the temperature at a distance x from the irradiated surface at a later time t is given by

$$\theta(x,t) = \frac{1}{L} \int_0^L \theta(x,0) dx + \frac{2}{L} \sum_{n=1}^{\infty} e^{-\frac{n^2 \pi^2}{L^2} Dt} \cos \frac{n\pi x}{L} \int_0^L \theta(x',0) \cos \frac{n\pi x'}{L} dx'. \quad (9)$$

Now, with $\theta(x',0)$ given by Eq. (4), Eq. (9) becomes

$$\theta(x,t) = \frac{A}{L} \left\{ (1 - e^{-aL}) + 2 \sum_{n=1}^{\infty} e^{-\frac{n^2 \pi^2}{L^2} Dt} \cos \frac{n\pi x}{L} \left[\frac{1 - (-1)^n e^{-aL}}{1 + \frac{n^2 \pi^2}{a^2 L^2}} \right] \right\}. \quad (10)$$

Again assuming $\theta(x,t) \ll T_0$, the single-ended back-scattering flash radiometry signal $S_B(t)$ given by Eq. (7) can be written as

$$S_B(t) = \frac{AK}{L} \left\{ (1-e^{-\alpha L})(1-e^{-\alpha' L}) + 2 \sum_{n=1}^{\infty} \left(\frac{1-(-1)^n e^{-\alpha L}}{1 + \frac{n^2 \pi^2}{\alpha^2 L^2}} \right) \left(\frac{1-(-1)^n e^{-\alpha' L}}{1 + \frac{n^2 \pi^2}{\alpha'^2 L^2}} \right) e^{-\frac{n^2 \pi^2}{L^2} Dt} \right\}. \quad (11)$$

In the conventional double-ended transmission measurement⁴ where the infrared detector is at the other side of the sample, the transmission radiometry signal $S_T(t)$ is

$$S_T(t) = K\alpha' \int_0^L e^{-\alpha'(L-x)} \theta(x,t) dx = \frac{AK}{L} \left\{ (1-e^{-\alpha L})(1-e^{-\alpha' L}) - 2e^{-\alpha' L} \sum_{n=1}^{\infty} e^{-\frac{n^2 \pi^2}{L^2} Dt} \left(\frac{1-(-1)^n e^{-\alpha L}}{1 + \frac{n^2 \pi^2}{\alpha^2 L^2}} \right) \left(\frac{1-(-1)^n e^{-\alpha' L}}{1 + \frac{n^2 \pi^2}{\alpha'^2 L^2}} \right) \right\}. \quad (12)$$

When α and α' are very large such that $\alpha L, \alpha' L \rightarrow \infty$, Eqs. (11) and (12) reduce to those given by Parker *et al.*¹. The signal $S(t)$ in general depends on α, α', L, D and is characterized by a characteristic time constant τ_L given by

$$\tau_L = \frac{L^2}{\pi^2 D}. \quad (13)$$

When $t > \tau_L$, only the first term inside the summations in Eqs. (11) and (12) is significant, and the infrared signals S_B and S_T both approach the same steady state value $\left(= \frac{AK}{L} (1-e^{-\alpha L})(1-e^{-\alpha' L}) \right)$ exponentially. Note that $S_B(t)$ approaches this steady state value from above and hence the back-scattering measurement intrinsically provides a higher

sensitivity than the transmission measurement in which the signal $S_T(t)$ approaches the steady state value from below. This advantage becomes more significant as the thickness of the sample is large.

Equation (11) should also reduce to Eq. (8) as the thickness L approaches infinite. In fact, we find that this is exactly the case (Appendix II). In other words, for $t \ll \tau_L = L^2/\pi^2 D$, the heat does not know the existence of the rear surface and the heat diffusion proceeds the same as in the semi-infinite case. Hence the early time development of $S(t)$ is mainly governed by α , α' and D , while in the later stage of the development, the length scale is replaced by the sample thickness L rather than α^{-1} and α'^{-1} . Figure 2(a) shows a plot of Eq. (8) (for semi-infinite solid) and Eq. (11) (for thin slab) with the same value of α, α' and D . The two curves practically overlap for $t \ll \tau_L$. As a result of this, we can determine the parameters α and α' of the sample by fitting the experimental data to Eq. (8) for $t \ll \tau_L$ if the thermal diffusivity D is known. On the other hand, if the thickness L and the absorption coefficients α and α' are known, the thermal diffusivity D can be determined by one-parameter fitting of Eqs. (11) or (12). In fact, we find that the thermal diffusivity D obtained by fitting experimental data with Eq. (11) is not sensitive to the value of α and α' if $\alpha L, \alpha' L \gg 1$ and if only data in the region $t > \tau_L$ are used. Figure 2(b) shows a plot of Eq. (11) with the same L but different α and α' . Although both α and α' are different by a factor of four in these two curves, the shape of the curves for $t > \tau_L$ are basically the same. This is quite obvious since from $t = \tau_L$ to $t = \infty$, the time decay of the signal is characterized by τ_L which is a function of L rather than α and α' . Further examination of Eqs. (8) and (11)-(12) reveals that α and α' are interchangeable without affecting the value of $S(t)$ which leads to an ambiguity in determining α and α' . However,

this uncertainty does not affect the thermal diffusivity D obtained by fitting Eqs. (8), (11) or (12).

C. Effects of Excitation Pulse Width and the Response Time of the Detecting System

When the excitation flash pulse is extended in time and has a magnitude proportional to $G(t)$, the signal $Z(t)$ at the infrared detector is equal to the convolution of $G(t)$ and $S(t)$,^{8,25} namely

$$Z(t) = \int_{-\infty}^{\infty} S(t-t')G(t')dt' . \quad (14)$$

In the case of thin slab sample and single-ended back-scattering radiometry measurement,

$$Z_B(t) = \frac{AK}{L}(1-e^{-\alpha L})(1-e^{-\alpha' L}) + \frac{2AK}{L} \sum_{n=1}^{\infty} \left(\frac{1-(-1)^n e^{-\alpha L}}{1 + \frac{n^2 \pi^2}{\alpha^2 L^2}} \right) \left(\frac{1-(-1)^n e^{-\alpha' L}}{1 + \frac{n^2 \pi^2}{\alpha'^2 L^2}} \right) \int_{-\infty}^{\infty} e^{-\frac{n^2 \pi^2}{L^2} D(t-t')} G(t') dt' . \quad (15)$$

When the excitation source is a pulsed laser, $G(t)$ can often be represented by a gaussian distribution, *i.e.*,

$$G(t) = \frac{2}{\Delta\sqrt{\pi}} e^{-4\left(\frac{t-t_0}{\Delta}\right)^2} \quad (16)$$

where t_0 is the time of maximum intensity and Δ is the pulse width. By putting Eq. (16) into (15), we obtain

$$Z_B(t) = \frac{AK}{L}(1-e^{-aL})(1-e^{-a'L}) + \frac{2AK}{L} \sum_{n=1}^{\infty} \left(\frac{1-(-1)^n e^{-aL}}{1 + \frac{n^2 \pi^2}{a^2 L^2}} \right) \left(\frac{1-(-1)^n e^{-a'L}}{1 + \frac{n^2 \pi^2}{a'^2 L^2}} \right) e^{\left(\frac{n^2 \pi^2 D \Delta}{4L^2} \right)^2 - \frac{n^2 \pi^2}{L^2} D(t-t_0)} \quad (17)$$

Similarly Eq. (12) for double-ended transmission radiometry measurement can be written as

$$Z_T(t) = \frac{AK}{L}(1-e^{-aL})(1-e^{-a'L}) - \frac{2AK}{L} e^{-a'L} \sum_{n=1}^{\infty} \left(\frac{1-(-1)^n e^{-aL}}{1 + \frac{n^2 \pi^2}{a^2 L^2}} \right) \left(\frac{1-(-1)^n e^{+a'L}}{1 + \frac{n^2 \pi^2}{a'^2 L^2}} \right) e^{\left(\frac{n^2 \pi^2 D \Delta}{4L^2} \right)^2 - \frac{n^2 \pi^2}{L^2} D(t-t_0)} \quad (18)$$

It is clear that from Eqs. (17) and (18), the correction due to the effect of flash pulse width is of second order in nature. If $\Delta \ll \tau_L (=L^2/\pi^2 D)$ the effect of pulse width can be neglected. Equations (17) and (18) are valid only if the observation time t is much larger than the flash pulse duration Δ (i.e., after the occurrence of the entire excitation pulse). For smaller t , the upper limit in the integral in Eq. (14) should be replaced by t .

The effect of the finite rise time of the detecting system (which includes the infrared detector, amplifier and data acquisition device) can also be analyzed in a similar way. The ultimate response $W(t)$ is equal to the convolution of the infrared signal $Z(t)$ and the impulse response $H(t)$ of the detecting system. In order to simplify the analysis, we approximate $H(t)$, the response of the detecting system to an impulse at $t=0$, by

$$H(t) = \frac{2}{\Delta' \sqrt{\pi}} e^{-4 \left(\frac{t-\Delta'}{\Delta'} \right)^2} \quad \text{for } t > 0,$$

where Δ' can be regarded as the rise time of the system. Hence, in single-ended back scattering radiometry measurement,

$$W_B(t) = \frac{AK}{L}(1-e^{-\alpha L})(1-e^{-\alpha' L}) + \frac{2AK}{L} \sum_{n=1}^{\infty} \left(\frac{1-(-1)^n e^{-\alpha L}}{1 + \frac{n^2 \pi^2}{\alpha^2 L^2}} \right) \left(\frac{1-(-1)^n e^{-\alpha' L}}{1 + \frac{n^2 \pi^2}{\alpha'^2 L'^2}} \right) e^{-\left(\frac{n^2 \pi^2}{4L^2} D \Delta' \right)^2 - \left(\frac{n^2 \pi^2}{4L^2} D \Delta \right)^2 - \frac{n^2 \pi^2}{L^2} D(t-t_0-\Delta')} \quad (19)$$

Similar expression can be written for $W_T(t)$, the final response in the transmission flash radiometry measurement. For $t \gg \Delta'$, the effect of the finite response time of the detecting system is not important.

EXPERIMENT

The experimental setup is very similar to that of our previous experiments^{15,16} (Fig. 3). A 1 mJ pulsed nitrogen laser (Molelectron UV12 nitrogen laser with $\lambda=337$ nm) of pulse width $\tau=8$ ns (full width at half maximum) is used as the excitation source. With such a short excitation pulse duration, the effect of the pulse width can be neglected in most cases. The laser beam is slightly focused to a spot size of around 4 mm \times 4 mm on the sample surface and the intensity of the laser pulse energy is suitably attenuated so that the *amplitude* of the detected infrared signal varies linearly with excitation energy (with the signal *shape* unchanged), and the approximation used in Eq. (7) is valid. The infrared signal emitted from the sample is collected by a concave mirror and is detected by a liquid N₂ cooled HgCdTe detector operating in photoconductive mode (New England Research Model

MPC12-2-J1). The detector is sensitive to 8-12 μm infrared radiation and has a rise time of about 0.5 μs . The rise times of other electronic devices in the detecting system are faster than 0.5 μs and hence may be neglected.

The experimental setup can be operated either in single-ended mode or double-ended mode, depending on the incident direction of the laser beam. Figure 4 shows signals obtained in single-ended back-scattering modes of operation for two pieces of black polyvinylchloride (PVC) film of 0.071 mm and 0.190 mm thicknesses. It is obvious that for small t , the lineshape of the two curves are identical (Fig. 4(a)). However, as t is larger than the characteristic time τ_L of the thin sample, deviation between the two curves becomes evident (Fig. 4(b)) as predicted by Eqs. (8) and (11).

We have used the method of least squares to fit the curve (i) of the 0.071 mm thick PVC tape using Eq. (11). Since the time used is much larger than 0.5 μs , corrections in excitation pulse duration and finite rise time of the detection system is not necessary. The final result is shown in Fig. 4(c). The average r.m.s. deviation of the theoretical fit (long dash line) and the experimental data (curve (i), solid line) is about 0.05, and the values of α , α' and D are found to be 833 cm^{-1} , 1000 cm^{-1} and 0.00135 cm^2/sec , respectively. As we mentioned in the last section, the values of α and α' can be interchanged without affecting the final result of D . In fact, the uncertainty of the fitted thermal diffusivity now mainly arises from the error in thickness measurement.

These fitted values of α , α' and D of the thin PVC film are used to calculate the line shape of the thick PVC film ($L=0.190$ mm) in the single-ended back-scattering measurement. The result is also shown in Fig. 4(c) with the theoretical fit represented by

short dash line and experimental data represented by solid line (curve (ii)). Again, the agreement between experimental data and theoretical prediction is excellent.

We have also carried out the conventional transmission flash radiometry measurements using the same samples. Figure 5(a) and (b) show typical results for the thin and thick samples, respectively. For the thin PVC sample (Fig. 5(a)), there is a jump in signal at small t , an indication of a leakage in either infrared or the excitation energy or both through the sample. This is also a good indication of the fact that the values of α and α' obtained earlier are not very large. For the thick sample (Fig. 5(b)), the signal starts to decay at around $t=160$ ms instead of remaining constant, an evidence that the heat loss effect becomes important. Using the previously obtained values of α , α' and D for the thin PVC film and Eq. (12), we are able to fit Figs. 5(a) and (b) with reasonably good agreement between experimental results and theoretical predictions (Fig. 5(c) and (d)). This is also an important experimental evidence that back-scattering single-ended flash radiometry measurements do get similar results as compared to the conventional transmission measurements, except that it is single-ended and has a higher intrinsic sensitivity.

To demonstrate the effect of the rise time in the detecting system, we have performed experiments on samples which have short τ_a , τ_a' , and τ_L . Figure 6(a) shows the single-ended back-scattering signal of a piece of 0.107 mm thick Co-Netic magnetic steel supplied by Magnetic Shield Division of Perfection Mica Company. The upper curve in Fig. 6(a) is the signal plus the background scatterings. The lower curve is the background scatterings obtained by putting a piece of glass slide in front of the infrared detector window so that the infrared signal is blocked but the scattered excitation pulse signal can still enter the detector. The true infrared signal is the difference between these two curves. Figure 6(b) shows the importance of the effect of the rise time of the detection system. The solid line is the true

infrared signal. The long-dash line is the best theoretical fit using Eq. (19) with the rise time $\Delta' = 0.85 \mu\text{s}$. The short-dash line is the fit using Eq. (11), which does not take into account of the effect of rise time. In these fits, the absorption coefficients α and α' are both taken to be 10^5 cm^{-1} which corresponds to a skin depth of approximately $0.1 \mu\text{m}$.

The effect of radiation heat loss has long been an important problem in flash radiometry and has been studied by many authors.^{3,5,6,8,13} They find that the effect of radiation heat loss is very important at high temperatures. Most of them also come up with complicated implicit expressions for the correction of radiation loss, which, however, are usually not very practical. Chen *et al.*¹³ has devised a feasible method based on the theoretical development of Cape and Lehmann.⁵ In their technique, two different time constants have to be measured, one being the characteristic time $\tau_L (= L^2 / \pi^2 D)$ of the sample, and the other being the decay time constant τ_R at $t \gg \tau_L$, which is mainly contributed by radiation heat loss and two-dimensional heat diffusion loss. From the ratio

$$\mu = \frac{\tau_L}{\tau_R}$$

they are able to determine the correction factor from a graph. For $\mu = 2\%$, the correction in the worse case is less than 4%. For our thin film sample, we find that τ_R is always at least two orders of magnitude larger than τ_L and hence the effect of radiation loss is negligible. Figures 7(a) and (b) show the signals a 0.071 mm thick black PVC film and a 0.0125 mm thick stainless steel sheet obtained in double-ended transmission flash radiometry measurement. τ_R is approximately several hundred milliseconds in both samples while τ_L is only around $4 \mu\text{s}$ for stainless steel and 3.7 ms for PVC tape.

Heat loss due to two-dimensional diffusion inside the sample has been considered by Lang.¹² He finds that when the ratio of the radius of the irradiated area to the sample thickness is greater than two, correction is not necessary. To prove this experimentally, we have cut small slits along the boundary of the irradiated area of the samples described in Fig. 7 so that the samples are supported at three points only and the lateral heat conduction loss should be greatly reduced. We found that, with these samples, the decay of the signal for large t is practically identical to Fig. 7. We then conclude the two-dimensional heat loss is negligible in our thin samples. The criterion of Lang can easily be satisfied for the thin film samples used in our experiments. For thicker samples, one can always defocus the laser beam so as to cover a larger sample area.

CONCLUSION

We have carried out detailed theoretical analysis on the lineshape of the signal in flash radiometry. In opaque thin samples when the time t is much smaller than the characteristic time τ_L , the heat diffuses as in the case of a homogeneous semi-infinite solid, and the decay of the signal are characterized by τ_α and $\tau_{\alpha'}$. When $t > \tau_L$, the signal decays in back-scattering radiometry (or rises in transmission radiometry) approximately exponentially to a steady state value with time constant τ_L . The thermal diffusivity D of the sample can be obtained more accurately by fitting the later part of the experimental data if α and α' are not known exactly. Finite excitation pulse duration and rise time of the detecting system are found to have approximately the same effect of delaying and broadening the signal. These theoretical predictions have been supported by experimental data. Radiation loss and two-dimensional diffusion loss are concluded negligible for thin samples at room temperature.

ACKNOWLEDGMENTS

This work is partially supported by the Office of Naval Research.

APPENDIX I

To carry out the integral (7) with $\theta(x,t)$ given by (5), one has to evaluate the following integral.

$$\int_0^x e^{-pu} \operatorname{erf}(qu) du. \quad (\text{A1})$$

Integration by parts and using the fact that

$$\frac{d}{du} (\operatorname{erf}(qu)) = \frac{2q}{\sqrt{\pi}} e^{-q^2 u^2},$$

Eq. (A1) becomes

$$\begin{aligned} \int_0^x e^{-pu} \operatorname{erf}(qu) du &= -\frac{e^{-px}}{p} \operatorname{erf}(qx) + \int_0^x \frac{2q}{p\sqrt{\pi}} e^{-pu - q^2 u^2} du \\ &= -\frac{e^{-px}}{p} \operatorname{erf}(qx) + \frac{e^{p^2/4q^2}}{p} \left[\operatorname{erf} q \left(x + \frac{p}{2q^2} \right) - \operatorname{erf} \frac{p}{2q} \right]. \end{aligned} \quad (\text{A2})$$

Equation (8) follows by applying (A2) several times. In the limit of $\alpha' \rightarrow \alpha$ (or $\alpha \rightarrow \alpha'$),

Eq. (8) can be reduced to

$$S(t) = AK\alpha \left\{ \left(\frac{1}{2} - \frac{t}{4\tau_\alpha} \right) \left(1 - \operatorname{erf} \sqrt{t/4\tau_\alpha} \right) e^{t/4\tau_\alpha} + \sqrt{t/4\pi\tau_\alpha} \right\}$$

using Taylor expansion about $\sqrt{t/4\tau_\alpha}$.

APPENDIX II

When $L \rightarrow \infty$, Eq. (11) can be written as

$$S_B(t) = \lim_{L \rightarrow \infty} AK \left\{ \frac{1}{L} + \frac{2}{L} \sum_{n=1}^{\infty} \left(\frac{1}{1 + \frac{n^2 \sigma^2}{\alpha^2 L^2}} \right) \left(\frac{1}{1 + \frac{n^2 \sigma^2}{\alpha'^2 L^2}} \right) e^{-\frac{n^2 \sigma^2}{L^2} Dt} \right\}. \quad (A3)$$

Let

$$u = \frac{n\sigma}{L}$$

$$\Delta u = \frac{\sigma}{L} \Delta n,$$

we then have

$$\begin{aligned} S_B(t) &= 2AK \lim_{L \rightarrow \infty} \frac{1}{L} \sum_{n=1}^{\infty} \left(\frac{1}{1 + \frac{u^2}{\alpha^2}} \right) \left(\frac{1}{1 + \frac{u^2}{\alpha'^2}} \right) e^{-Du^2 \frac{L}{\sigma}} \Delta u \\ &= \frac{2AK}{\sigma} \int_0^{\infty} \frac{e^{-Du^2}}{\left(1 + \frac{u^2}{\alpha^2}\right) \left(1 + \frac{u^2}{\alpha'^2}\right)} du \\ &= \frac{2AK\alpha\alpha'}{\sigma} \int_0^{\infty} \frac{1}{(\alpha'^2 - \alpha^2)} \left\{ \frac{1}{(\alpha^2 + u^2)} - \frac{1}{(\alpha'^2 + u^2)} \right\} e^{-Du^2} du. \end{aligned} \quad (A4)$$

Direct integration of (A4) will lead to Eq. (8). The signal $S_T(t)$ in the limit of $L \rightarrow \infty$ in the double-ended transmission flash radiometry measurement can be obtained similarly.

REFERENCES

1. W. J. Parker, R. J. Jenkins, C. P. Butler and G. L. Abbott, *J. Appl. Phys.* 32, 1679 (1961).
2. R. D. Cowan, *J. Appl. Phys.* 32, 1363 (1961).
3. W. J. Parker and R. J. Jenkins, *J. Appl. Phys.* 2, 87, (1962).
4. H. W. Deem and W. D. Wood, *Rev. Sci. Instrum.* 33, 1107 (1962).
5. J. A. Cape and G. W. Lehman, *J. Appl. Phys.* 34, 1909 (1963).
6. R. Taylor, *Brit. J. Appl. Phys.* 16, 509 (1965).
7. D. Shaw and L. A. Goldsmith, *J. Sci. Instrum.* 43, 594 (1966).
8. D. A. Watt, *Brit. J. Appl. Phys.* 17, 231 (1966).
9. K. B. Larson and K. Koyama, *J. Appl. Phys.* 39, 4408 (1968).
10. H. J. Lee and R. E. Taylor, *J. Appl. Phys.* 47, 148 (1976).
11. J. A. McKay and J. T. Schriempt, *J. Appl. Phys.* 47, 1668 (1976).
12. S. B. Lang, *Ferroelectrics* 11, 315 (1976).
13. F. C. Chen, Y. M. Poon and C. L. Choy, *Polymer* 18, 129 (1977).
14. A. Cruz-Urbe and J. U. Trefny, *J. Phys. E* 15, 1054 (1982).
15. A. C. Tam and B. Sullivan, *Appl. Phys. Lett.* 43, 333 (1983).
16. W. P. Leung and A. C. Tam, *Optic Letters* (accepted for publication).
17. H. S. Carslaw and J. C. Jaeger, "Conduction of Heat in Solids," 2nd edition (Clarendon, Oxford, 1959), p. 56 and p. 359.
18. P. E. Nordal and S. O. Kanstand, *Physica Scripta* 20, 659 (1979).
19. S. O. Kanstad and P. E. Nordal, *Appl. Surf. Sci.* 6, 372 (1980).
20. P. E. Nordal and S. O. Kanstad, *Appl. Phys. Lett.* 38, 486 (1981).
21. G. Busse, *Infrared Phys.* 20, 419 (1980).
22. R. Santog and L. C. M. Miranda, *J. Appl. Phys.* 52, 4194 (1981).

23. R. D. Tom, E. P. O'Hara and D. Benin, *J. Appl. Phys.* **53**, 5392 (1982).
24. H. S. Carslaw and J. C. Jaeger, "Conduction of Heat in Solid," 2nd edition (Clarendon, Oxford, 1959), p. 101.
25. J. W. Goodman, *Introduction to Fourier Optics* (McGraw-Hill, New York, 1968).

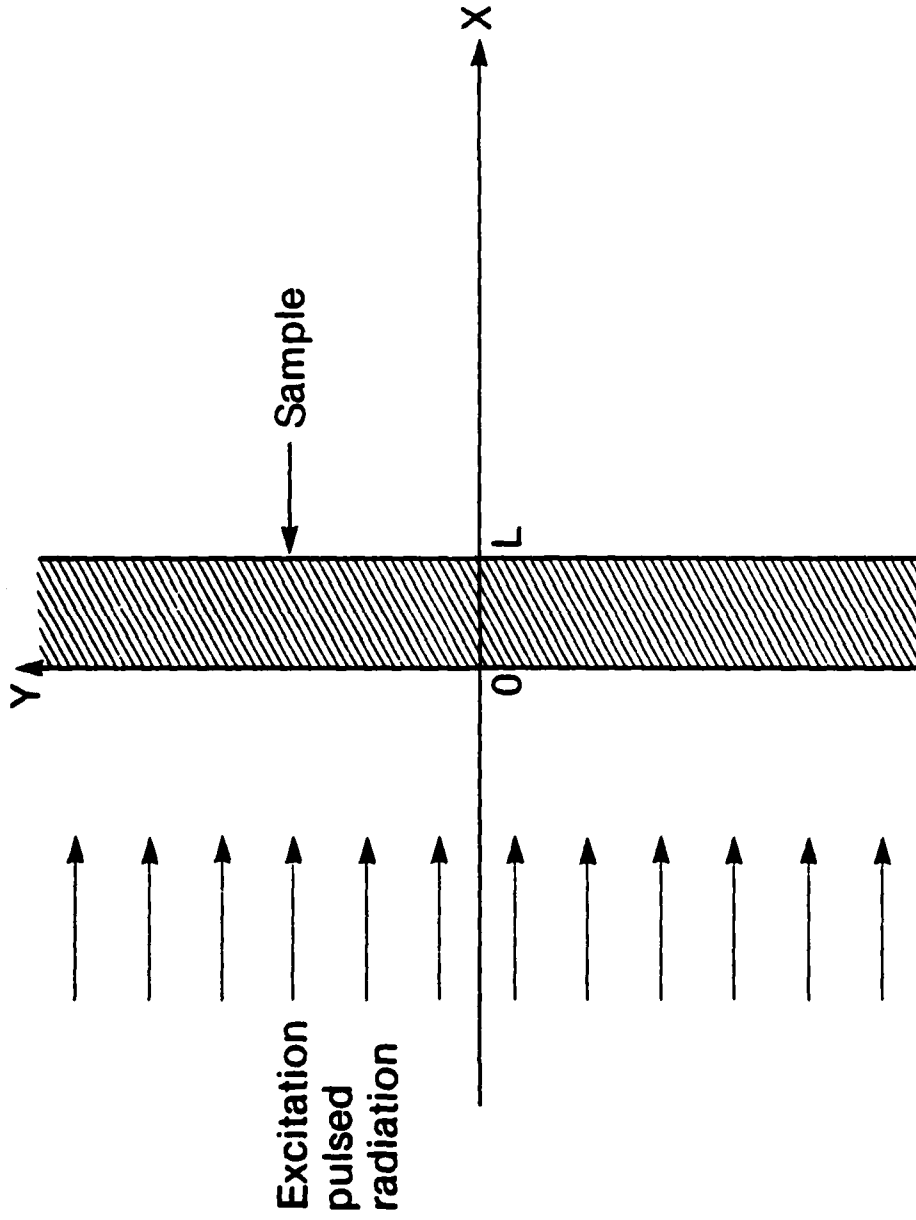


Figure 1. Schematic diagram for a thin solid sample.

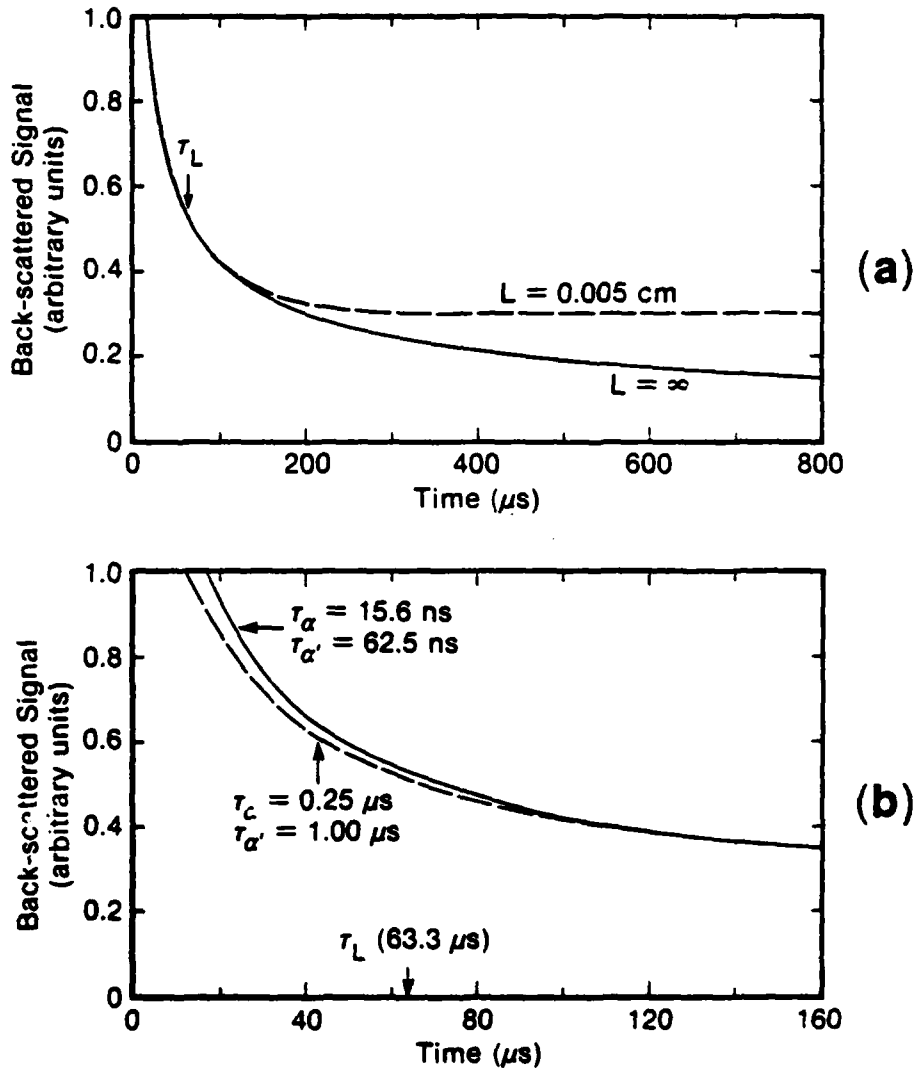


Figure 2. Theoretical response of the single-ended back-scattering flash radiometry signal. (a) Effect of sample thickness: dash line $L = 0.005 \text{ cm}$; solid line $L = \infty$. In both curves, α , α' and D are taken as $2 \times 10^4 \text{ cm}^{-1}$, $1 \times 10^4 \text{ cm}^{-1}$ and $0.04 \text{ cm}^2/\text{s}$, respectively. These are typical values for stainless steel. (b) Effect of α and α' : dash line, $\alpha = 5 \times 10^3 \text{ cm}^{-1}$, $\alpha' = 2.5 \times 10^3 \text{ cm}^{-1}$; solid line, $\alpha = 2 \times 10^4 \text{ cm}^{-1}$, $\alpha' = 1 \times 10^4 \text{ cm}^{-1}$. In both curves, L and D are taken as 0.005 cm and $0.04 \text{ cm}^2/\text{s}$, respectively.

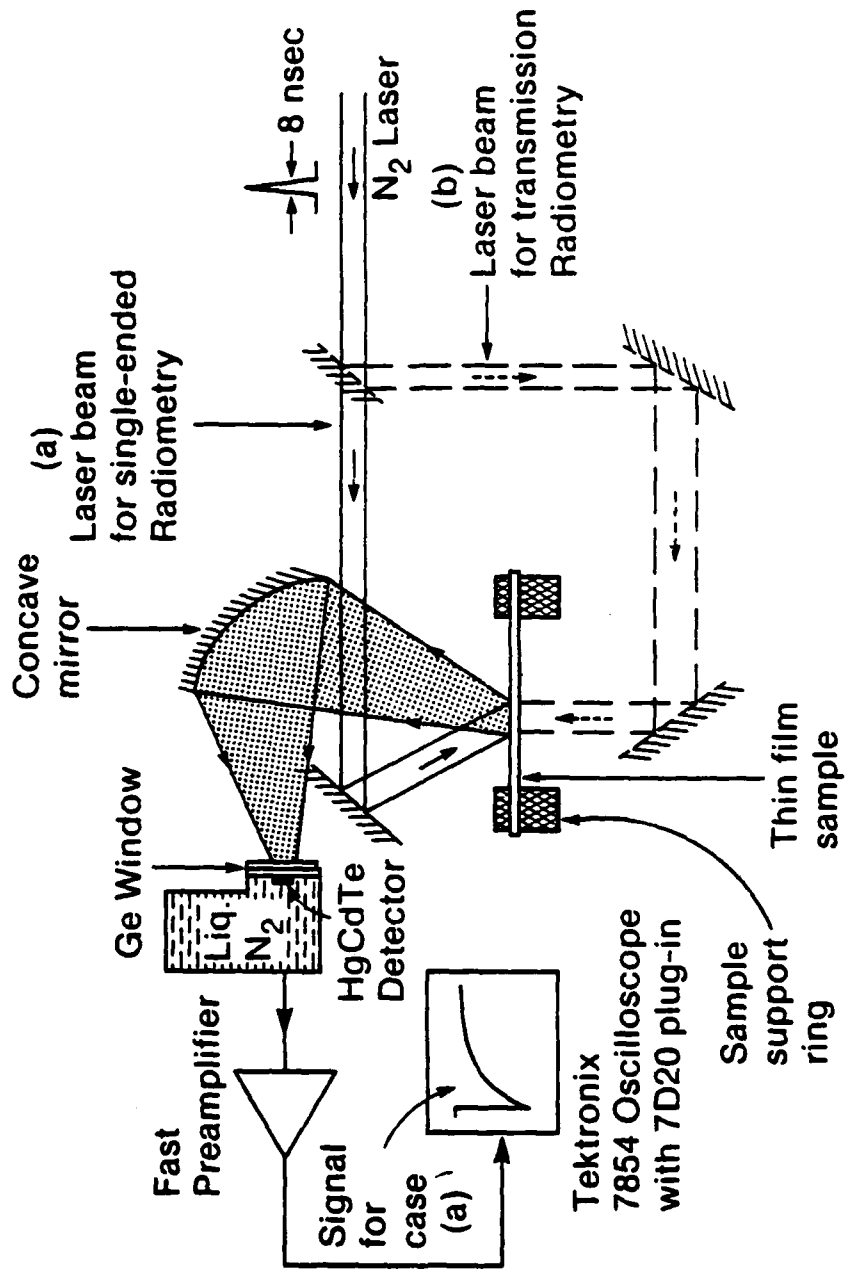


Figure 3. Experimental setup for both single-ended back-scattering (laser beam represented by solid lines) and double-ended (laser beam represented by dash lines) transmission radiometry measurements.

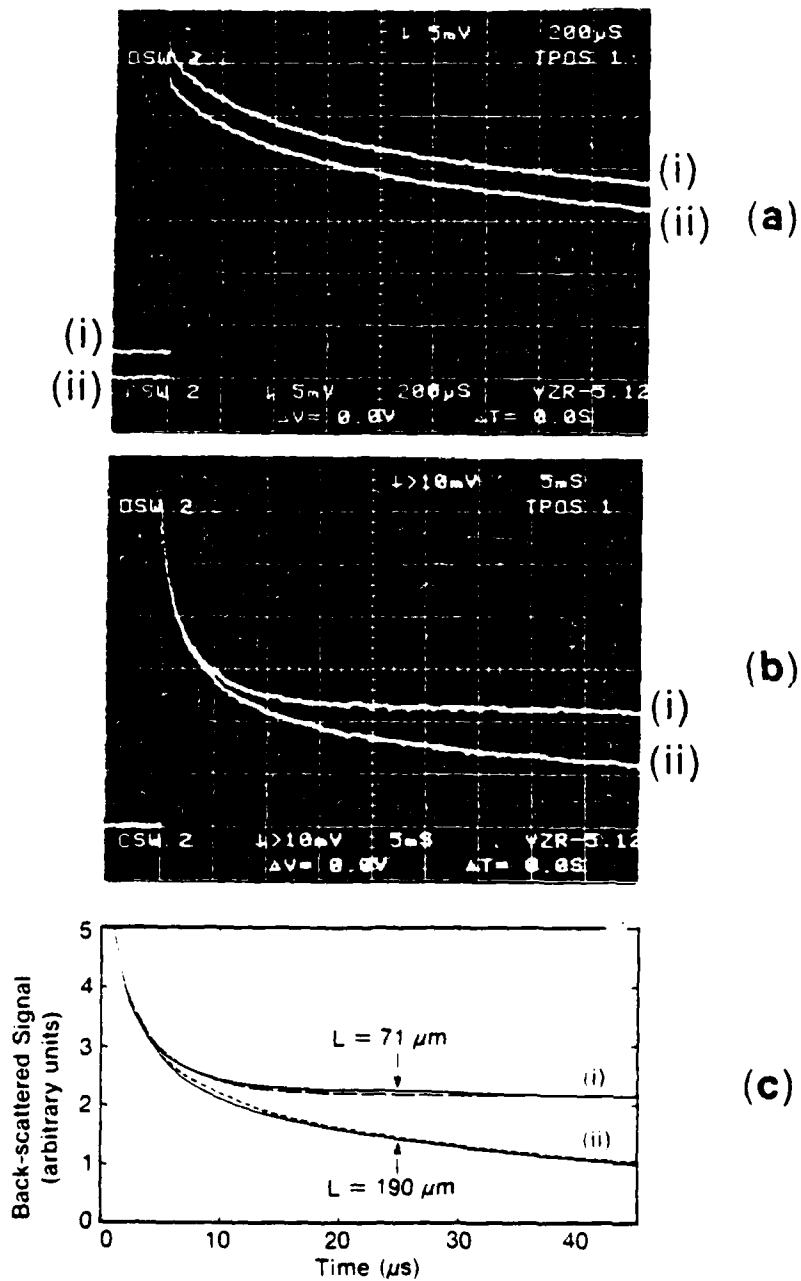


Figure 4. Back-scattering radiometry signal for black PVC films. Curve (i), $L = 71 \mu\text{m}$, curve (ii), $L = 190 \mu\text{m}$. (a) and (b), experimental results, (c) Theoretical fits: long-dash line, $L = 71 \mu\text{m}$; short-dash line: $L = 190 \mu\text{m}$.

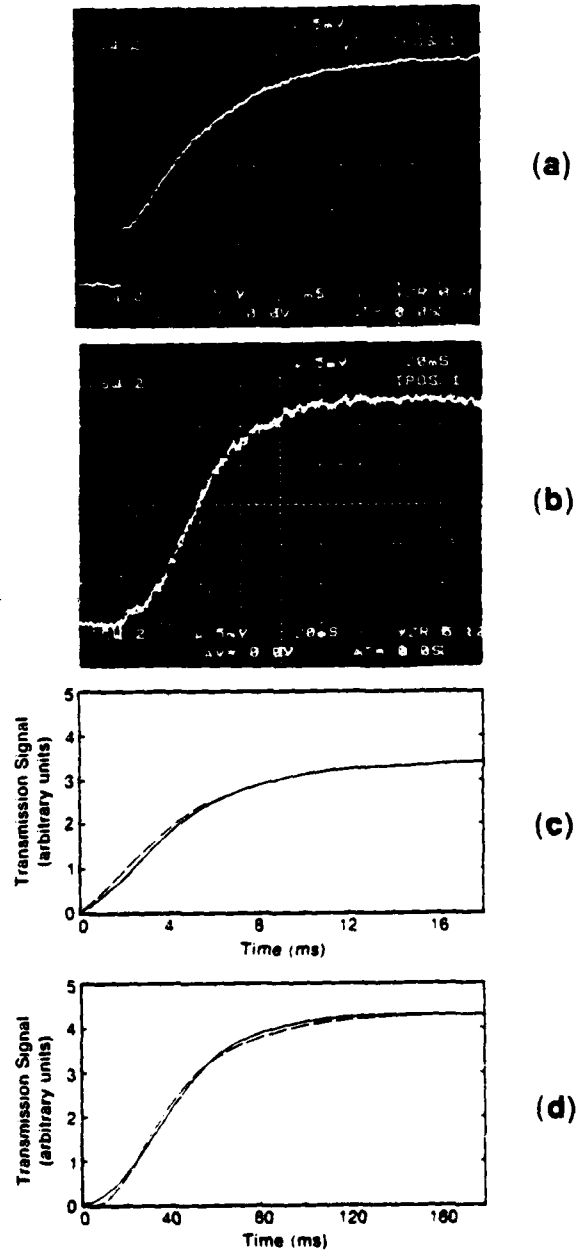


Figure 5. Transmission radiometry signal for black PVC films. (a) Experimental result, $L=71 \mu\text{m}$; (b) Experimental result, $L=190 \mu\text{m}$; (c),(d) Theoretical fits for (a) and (b), respectively, using the values of α , α' and D obtained in Fig. 4(c) for $L=71 \mu\text{m}$.

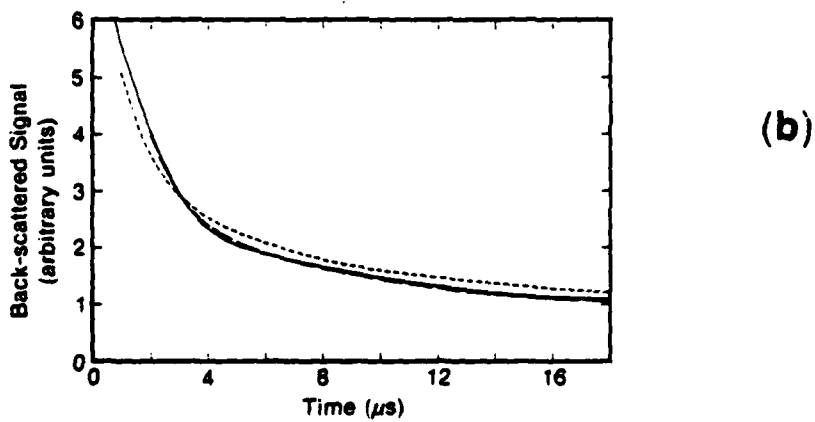
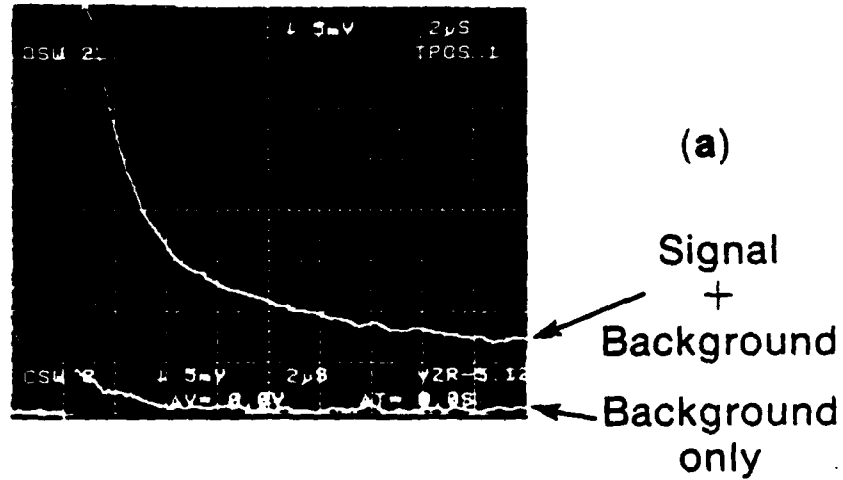
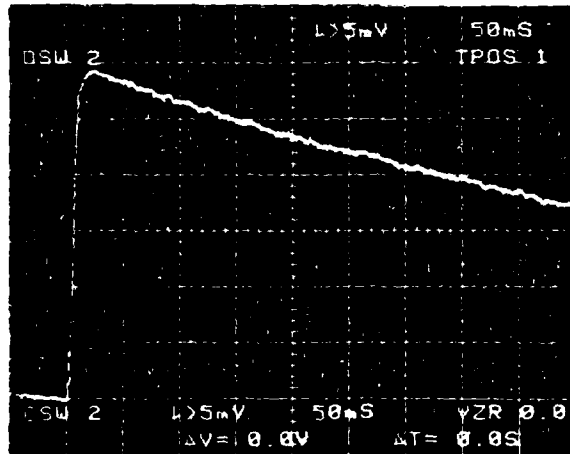
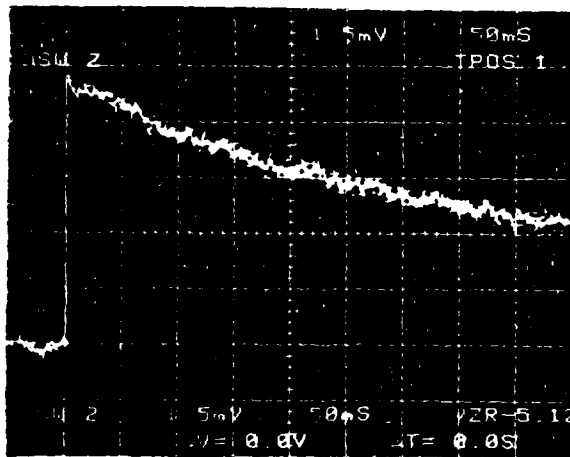


Figure 6. (a) Back-scattering radiometry signal for a piece of $107 \mu\text{m}$ thick Co-Netic magnetic steel. (b) Theoretical fits of (a) using Eq. (19) (long-dash line) and Eq. (11) (short-dash line). The solid line is the true experimental infrared signal obtained by subtracting the two curves in (a).



(a)



(b)

Figure 7. Observed transmission radiometry signal of a piece of 71 μm thick black PVC film (a) and a piece of 12.5 μm thick stainless steel sheet (b). The decay of the signals is mainly due to convection and radiation heat loss.

short dash line and experimental data represented by solid line (curve (ii)). Again, the agreement between experimental data and theoretical prediction is excellent.

We have also carried out the conventional transmission flash radiometry measurements using the same samples. Figure 5(a) and (b) show typical results for the thin and thick samples, respectively. For the thin PVC sample (Fig. 5(a)), there is a jump in signal at small t , an indication of a leakage in either infrared or the excitation energy or both through the sample. This is also a good indication of the fact that the values of α and α' obtained earlier are not very large. For the thick sample (Fig. 5(b)), the signal starts to decay at around $t=160$ ms instead of remaining constant, an evidence that the heat loss effect becomes important. Using the previously obtained values of α , α' and D for the thin PVC film and Eq. (12), we are able to fit Figs. 5(a) and (b) with reasonably good agreement between experimental results and theoretical predictions (Fig. 5(c) and (d)). This is also an important experimental evidence that back-scattering single-ended flash radiometry measurements do get similar results as compared to the conventional transmission measurements, except that it is single-ended and has a higher intrinsic sensitivity.

To demonstrate the effect of the rise time in the detecting system, we have performed experiments on samples which have short τ_a , τ_a' , and τ_L . Figure 6(a) shows the single-ended back-scattering signal of a piece of 0.107 mm thick Co-Netic magnetic steel supplied by Magnetic Shield Division of Perfection Mica Company. The upper curve in Fig. 6(a) is the signal plus the background scatterings. The lower curve is the background scatterings obtained by putting a piece of glass slide in front of the infrared detector window so that the infrared signal is blocked but the scattered excitation pulse signal can still enter the detector. The true infrared signal is the difference between these two curves. Figure 6(b) shows the importance of the effect of the rise time of the detection system. The solid line is the true

infrared signal. The long-dash line is the best theoretical fit using Eq. (19) with the rise time $\Delta' = 0.85 \mu\text{s}$. The short-dash line is the fit using Eq. (11), which does not take into account of the effect of rise time. In these fits, the absorption coefficients α and α' are both taken to be 10^5 cm^{-1} which corresponds to a skin depth of approximately $0.1 \mu\text{m}$.

The effect of radiation heat loss has long been an important problem in flash radiometry and has been studied by many authors.^{3,5,6,8,13} They find that the effect of radiation heat loss is very important at high temperatures. Most of them also come up with complicated implicit expressions for the correction of radiation loss, which, however, are usually not very practical. Chen *et al.*¹³ has devised a feasible method based on the theoretical development of Cape and Lehmann.⁵ In their technique, two different time constants have to be measured, one being the characteristic time $\tau_L (=L^2/\pi^2D)$ of the sample, and the other being the decay time constant τ_R at $t \gg \tau_L$, which is mainly contributed by radiation heat loss and two-dimensional heat diffusion loss. From the ratio

$$\mu = \frac{\tau_L}{\tau_R}$$

they are able to determine the correction factor from a graph. For $\mu = 2\%$, the correction in the worse case is less than 4%. For our thin film sample, we find that τ_R is always at least two orders of magnitude larger than τ_L and hence the effect of radiation loss is negligible. Figures 7(a) and (b) show the signals a 0.071 mm thick black PVC film and a 0.0125 mm thick stainless steel sheet obtained in double-ended transmission flash radiometry measurement. τ_R is approximately several hundred milliseconds in both samples while τ_L is only around $4 \mu\text{s}$ for stainless steel and 3.7 ms for PVC tape.

MED
8